JPE 6-2-9

A Sliding Mode Observer Design for Fuel Cell Electric Vehicles

Induck Park† and Sikyung Kim*

†*Dept. of Electrical Eng., Kongju National University, Kongju, Korea

ABSTRACT

This paper presents the sliding mode observer of an induction motor for the fuel cell electric vehicles. The exact rotor flux estimation of the induction motor is important for achieving the best performance from the fuel cell electric vehicle system. However, the flux estimator of the induction motor control is highly sensitive to the voltage sensor output characteristics and system parameter variation influenced by external factors. In order to eliminate these problems, this paper investigates the electric vehicle performance due to parameter variation of the induction motor. A new method to estimate the fuel cell electric vehicle system is proposed based on the sliding mode observer.

Keywords: Sliding Mode Observer, Fuel Cell, Induction Motor, Electric Vehicle

1. Introduction

Today, millions of people depend on the automobile as their main source of transportation. The internal combustion engine causes air pollution, acid rain, and the buildup of greenhouse gases in the atmosphere. On the other hand, fuel cell systems produce little or no polluting emissions. Fuel cells are also more efficient than the internal combustion engine, and utilize hydrogen, which can be obtained from renewable resources.

This paper presents the sliding mode observer of an induction motor for fuel cell electric vehicles. Furthermore, the investigation of the electric vehicle performance under the parameter variation of the induction motor has been carried. The simulation results demonstrate that the proposed new method could successfully estimate the performance of the fuel cell electric vehicle based on the sliding mode observer. The exact rotor flux estimation of the induction motor is very essence to achieve the best performance from the fuel cell electric vehicle. However, the flux estimator of the induction motor controller is highly sensitive to the sensors' characteristics and system parameter variations influenced by the external environment. Therefore, this paper presents the novel method to minimize side effects due to parameter variation of the induction motor.

Manuscript received January 14, 2005; revised March 9, 2006
†Corresponding Author: han7770@kongju.ac.kr
Tel: +82-041-850-8835, Kongju National University
*Dept. of Electrical Eng. Kongju National University

2. Fuel Cell Vehicles

Currently, most fuel cell vehicles are classified into two categories [1]: the vehicles with battery energy storage and the vehicles without battery storage. In systems with battery storage, a DC/DC converter in the front end of the power electronics interface changes the low voltage input of the fuel cell to the higher level. A battery bank used in parallel connected with DC-link enables the most effective use of energy of the fuel cell as well as that of the batteries.

Battery provides the rapid start-up time and the faster

response for sudden road load change. The main disadvantage is the huge size of the battery bank, which leads to charge balance problems. The circuitry for equalizing the battery pack increases the cost, especially when the battery-pack voltage level is high[2]. The fuel cell system without battery has reduced size and cost but has to sacrifice many advantages of the first system. The vehicles cannot start-up instantly, require preheating arrangement, and cannot quickly response to sudden road load change. Moreover, a 12V auxiliary battery is required to supply the power to the accessory loads to start the fuel cell system.

These characteristics lead to the conclusion that the configuration with battery is the most suitable for the electric vehicle system. The question becomes where the battery should be located in the system. Placing the battery bank after the DC/DC converter adds cost, weight and size to the system. The present research proposes a topology where the battery with a control switch is set in the low voltage stage along with the fuel cell.

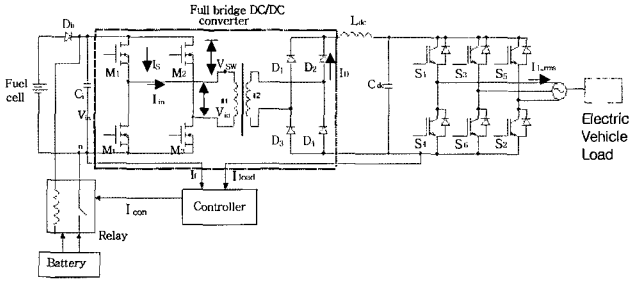

Fig. 1 Fuel cell electric vehicle

Figure 1 shows a suitable fuel cell vehicle topology, where a battery connected with a control switch is utilized in the input along with the fuel cell. In this configuration, the battery voltage will be the same as the nominal voltage of the fuel cell. For example, if a 48V proton exchange membrane (PEM) fuel cell (the fuel cell with high voltage is not efficient) is used, the battery voltage will be 48V. Since the battery is recharged at a low current during normal operation of the fuel cell, the power ratings of charging capacitor and diode are low which will minimize the cost. The purpose of the diode is to prevent the flow of current from battery to fuel cell. The battery comes in operation during start-up of the transient fuel cell and under the sudden road changes, since the fuel cell transient response is extremely slow. Since a small battery bank is used, this configuration reduces cost, weight and size significantly, while eliminating battery charge equalizing problems. Therefore, the topology in Figure 1 is suitable for the fuel cell electric vehicle.

2.1 Power conversion stages

In fuel cell electric vehicle, the DC/DC converter is a critical unit since it boosts up low fuel cell voltage. A PEM fuel cell is the most promising fuel cell technology that is suitable for transportation applications. PEM technology is gaining importance in automotive applications for its high power density, low temperature operation (which leads to rapid start-up time), low manufacturing cost and ability to withstand the shock and vibrations of the automotive environment[1,3]. The power cannot flow in reverse direction from dc-link to fuel cell, since the fuel cell remains on the uncharged status. Therefore, a unidirectional DC/DC converter is sufficient to serve this purpose. Moreover, a unidirectional DC/DC converter reduces the complexity in the control system. There are three standard high power DC/DC converters (Full-bridge, Half-bridge and Push-pull), which can be used for fuel cell vehicle. For the same input voltage, the switches carry twice as much current in the half-bridge compared with the full-bridge converter[4], which increases the number of parallel devices in the switches of the half-bridge converter. In a push-pull converter, the switches carry the same current as full-bridge switches. The full-bridge DC/DC converter requires fewer parallel devices in the switch configuration, smaller size of transformer, and has less core saturation probability. During braking time of the vehicle and the dead time of the inverter switches, the DC-link capacitor should absorb the regenerative power. The ultra capacitor can be utilized to aim this purpose, since this type of capacitor has the higher energy density compared to other types of capacitor.

Power processing unit is composed of a universal three-phase inverter that is operated on a high frequency, and a low loss performance. The fuel cell response time to changes is on the order of 90sec [2,5]. The use of a battery pack is required to solve the transient problem of the system due to the slow response of the fuel cell.

2.2 Electric Vehicle load

The road load for an electric vehicle consists of gravitational force, rolling resistance of the tires, and the aerodynamic drag force[6].

$$F_{RL} = F_{gxT} + F_{roll} + F_{AD} \tag{1}$$

where xT is the tangential direction along the roadway. The tractive force F_{TR} provided by the propulsion unit of the vehicle must overcome the road load force F_{RL} to propel the vehicle at a desired velocity. Figure 2 shows the forces acting on the vehicle.

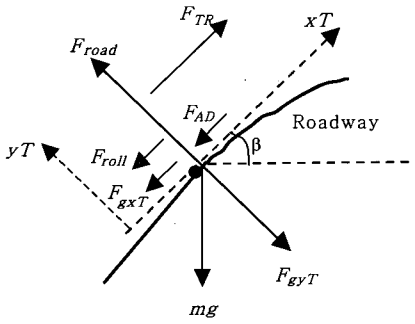

Fig. 2 Forces acting on vehicle

The gravitational force depends on the slope of the roadway.

$$F_{gxT} = mg \sin \beta \tag{2}$$

where m is the total mass of the vehicle, g is the gravitational acceleration constant and β is the grade angle with respect to horizon.

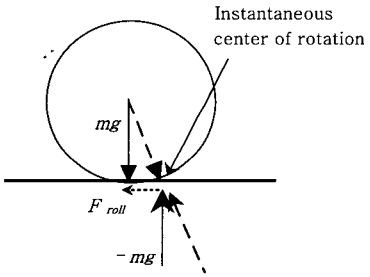

Fig. 3 Rolling resistance force of wheels

The tire on the contact surface produces the rolling resistance. The rolling resistance force is the component force of the vertical load mg, which is tangential to the roadway as shown in Figure 3. The tractive force F_{TR} must overcome the tangential force F_{roll} along with the gravitational force and the aerodynamic drag force. The ratio of the retarding force and the vertical load on the wheel is known as the coefficient of rolling resistance C_0. The rolling resistance force is given by

$$F_{roll} = \begin{cases} \text{sgn}[v_{xT}]mg(C_0 + C_1 v_{xT}^2) & \text{if} \quad v_{xT} \neq 0 \\ (F_{gxT} + F_{TR}) & \text{if} \quad v_{xT} \neq 0 \ \left|F_{gxT} + F_{TR}\right| \leq C_0 mg \\ \text{sgn}[F_{gxT} + F_{TR}](C_0 mg) & \text{if} \quad v_{xT} \neq 0 \text{ and } \left|F_{gxT} + F_{TR}\right| \leq C_0 mg \end{cases} \tag{3}$$

Typically $0.004 < C_0 < 0.02$ (unitless) and $C_1 << C_0$ (sec^2/m^2). v_{xT} are in *m/sec*. The aerodynamic drag force is the viscous resistance of the air working against the motion of the vehicle. The force is given by

$$F_{AD} = \text{sgn}[v_{xT}]\{0.5\rho C_D A_F (v_{xT} + v_0)^2\} \tag{4}$$

where ρ is the air density in kg/m^3, C_D is the aerodynamic drag coefficient (dimensionless, which typically is $0.2 < C_D < 0.4$), A_F is the equivalent frontal area of the vehicle, and v_0 is the head-wind velocity.

2.3 Induction Motor Control

The significance of the squirrel cage induction motors in speed and position controlled drives have grown drastically because of the large-scale application of AC induction motors in the industry. The induction motor, which is used in vehicle propulsion system, is controlled by the indirect method of vector control. The torque of the motor together with the electric vehicle load can be written as the following equation:

$$T_e = J\frac{dw_m}{dt} + Bw_m + T_{EV} \tag{5}$$

where w_m is the angular velocity of the rotor in rad/sec, J is the moment of inertia of the system, and B is the viscous coefficient of the motor. The electric vehicle torque T_{EV} can be obtained from the tractive force F_{TR} and wheel radius r_{wh} of the vehicle as the following equation:

$$T_{EV} = F_{TR} \cdot r_{wh} \tag{6}$$

The electromagnetic torque T_e generated from indirect vector control of the induction motor can be expressed as:

$$T_e = \frac{3}{2}\left(\frac{P}{2}\right)\frac{L_m}{L_r} i_{qs}\hat{\psi}_r \tag{7}$$

where P is the number of poles, L_m is the mutual inductance, and L_r is the rotor self inductance. i_{qs} and $\hat{\psi}_r$ are the quadrature components of the stator current and the rotor flux, respectively.

3. Sliding Mode Observer for Electric Vehicle Induction Motor

The following equations show the induction motor's behavior on electric vehicles in the stationary frame.

$$\begin{aligned}\frac{d}{dt}\begin{bmatrix} i_s \\ \phi_r \end{bmatrix} &= \begin{bmatrix} A_{11} & A_{12} \\ A_{21} & A_{22} \end{bmatrix}\begin{bmatrix} i_s \\ \phi_r \end{bmatrix} + \begin{bmatrix} B_1 \\ 0 \end{bmatrix} v_s \\ &= A_x + Bv_s \\ i_s &= C_x \end{aligned} \tag{8}$$

where

$i_s = [i_{ds} i_{qs}]^T$ stator current

$\phi_r = [\phi_{dr} \phi_{qr}]^T$ rotor flux

$v_s = [v_{ds} v_{qs}]^T$ stator voltage

$A_{11} = -\{R_s/(\sigma L_s) + (1-\sigma)/(\sigma\tau_r)\}I = a_{r11} I$

$A_{12} = M/(\sigma L_s L_r)\{(1/\tau_r)I - \varpi_r J\} = a_{r12} I + a_{i12} J$

$A_{21} = (M/\tau_r)I = a_{r21} I$

$A_{22} = -(1/\tau_r)I + \varpi_r J = a_{r22} I + a_{i22} J$

$B_1 = 1/(\sigma L_s) I = b_1 I$

$C = [I \quad 0]$

$I = \begin{bmatrix} 1 & 0 \\ 0 & 1 \end{bmatrix}$ $J = \begin{bmatrix} 0 & -1 \\ 1 & 0 \end{bmatrix}$

R_s, R_r stator and rotor resistance

L_s, L_r stator and rotor self inductance

M mutual inductance

σ leakage coefficient, $\sigma = 1 - M^2/(L_s L_r)$

τ_r rotor time constant, $\tau_r = L_r / R_r$

ϖ_r motor angular velocity

In the indirect field oriented control, the slip relation is employed to obtain the correct subdivision of the stator current into the torque and flux components. To incorporate perfect static and dynamic qualities of these drives, it is necessary to know the parameter variation effects in a induction motor. If the time constant of the rotor open circuit is constant, L_r/r_r (L_r and r_r are the rotor inductance and resistance, respectively) is not correctly known, or if it changes because of motor heating, skin effect or other variations, the subdivision of the stator current will not be correctly attained. The result will be detuning of the controller as a loss of correct field orientation[7,8]. This detuning causes incorrect calculation of the rotor field angle, and incorrect stator current component with the result that[9] (1) The flux level is not properly maintained, (2) the resulting steady state torque is not the commanded value, and (3) the torque response is not instantaneous. This paper presents a sliding observer to eliminate the effects of parameter variation for an electric vehicle under the varying load. The following equation describes the sliding observer which estimates the stator current and the rotor flux:

$$\frac{d}{dt}\hat{x} = \hat{A}\hat{x} + Bv_s + L(\hat{i}_s - i_s) + Ksign(\hat{i}_s - i_s) \tag{9}$$

where ^ means the estimated values, **L** is the observer gain matrix which is decided so that (9) can be stable, and sign is signum function. The sliding observer gain K has been chosed with large value enough to guarantee the sling mode. For the speed estimation, the adaptive scheme obtained from the Lyapunov function has been utilized [11].

$$\hat{\varpi}_r = K_p(e_{ids}\hat{\phi}_{qr} - e_{iqs}\hat{\phi}_{dr}) + K_I\int(e_{ids}\hat{\phi}_{qr} - e_{iqs}\hat{\phi}_{dr})dt \tag{10}$$

where $\hat{\phi}_{qr}, \hat{\phi}_{dr}$ is obtained from the equation (9). From the above equation, the electric vehicle speed could be estimated.

4. Simulation Results

Simulation for a fuel cell vehicle with 17kW load has been carried out utilizing the Matlab-Simulink power system toolbox to analyze the electrical characteristics of the power conversion stages. The effects for the parameter variation of the motor have been observed through the simulation study. In simulation, six real switches (IGBT) are used for the three-phase inverter, and a hysteresis current regulator is used for current regulation. The velocity profile of the electric vehicle applied in simulation is the urban driving cycle of the SAE J227a driving schedule B[10]. The maximum speed, acceleration time and cruise time are 20mph, 19sec and 19sec, respectively. The specifications of the electric vehicle load and the induction motor are given in Table 1.

Figure 4 shows the simulation results of the induction motor for the electric vehicle. Figure 5 shows the simulation results for the sliding observer. From the Figure 4 (a) and 5(a), it is observed that the estimated speed profile follows the SAE schedule B. Figure 5(b),(c),(d), and (e) show the d-axis current (i_{ds}), q-axis current (i_{qs}), the q-axis flux (ϕ_{qr}), and d-axis flux(ϕ_{dr}) respectively. The estimated $\hat{i}_{ds}$, $\hat{i}_{qs}$, $\hat{\phi}_{d}$, and $\hat{\phi}_{q}$ waveforms are presented in Figure 5(b),(c),(d), and (e). From Figures 4 and 5, it is found that the estimated currents and flux well follow up the actual currents and flux.

Table 1 The specifications of the electric vehicle load and the induction motor

Vehicle speed	20mph
Vehicle mass	500Kg
Rolling resistance coefficients C_0, C_1	0.009, 1.7E-6
Aerodynamic drag coefficient C_D	0.2
Vehicle frontal area A_F	$2m^2$
Rotational inertia coefficient K_m	1.1
Transmission gear ratio	10
Wheel radius r_{wh}	0.28m
Induction motor	60KW, 280V, 4 pole, 60Hz
Rotor resistance, inductance	0.228Ω, 0.8e-3H
Stator resistance, inductance	0.087Ω, 0.8e-3H
Mutual inductance	34.7e-3H
Moment of inertial	1.662 kg-m^2

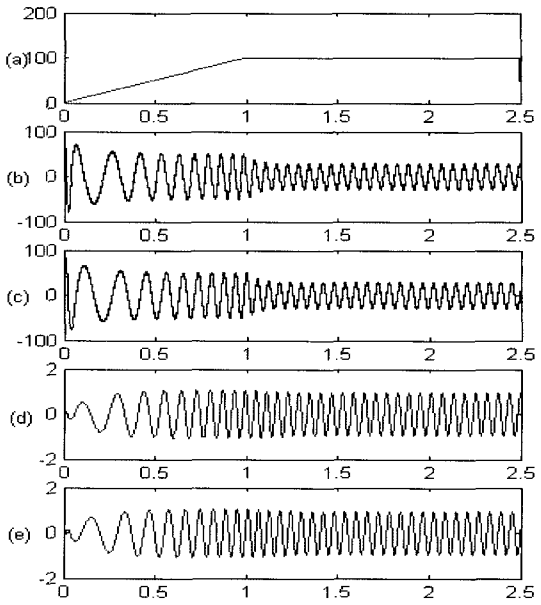

Fig. 4 Vector control simulation waveforms
(a) ω_r Actual Speed
(b) i_{ds} d-axis Current
(c) i_{qs} q-axis Current
(d) ϕ_{dr} d-axis Flux
(e) ϕ_{qr} q-axis Flux

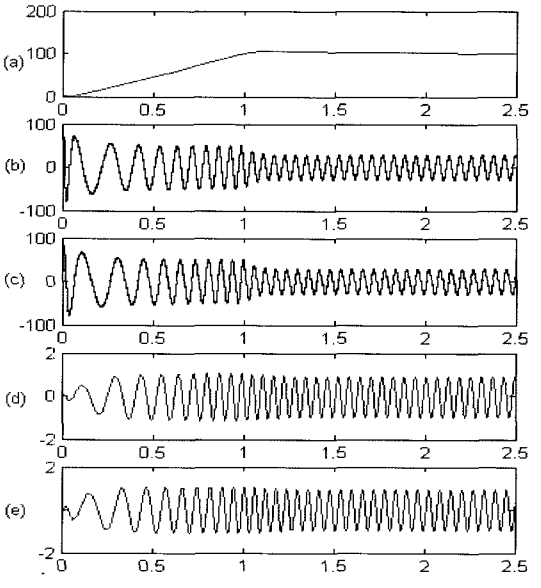

Fig. 5 Sliding mode observer simulation waveforms
(a) $\hat{\omega}_r$ Estimated speed with Sliding Observer
(b) i_{ds} Estimated d-axis Current
(c) i_{qs} Estimated q-axis Current
(d) ϕ_{d} Estimated d-axis Flux
(e) ϕ_{q} Estimated q-axis Flux

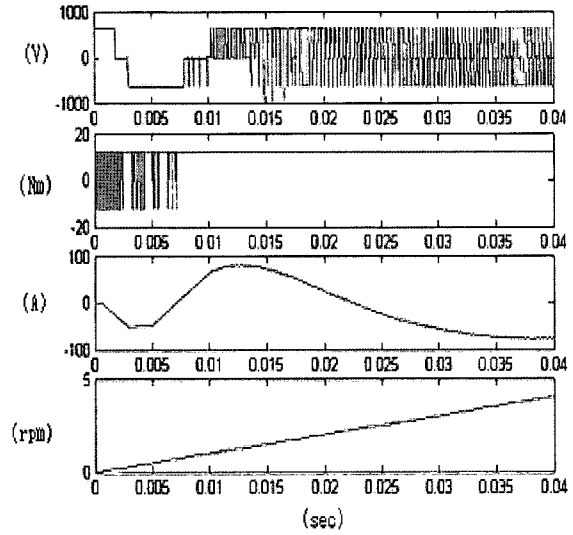

Fig 6 Torque change to 3Phase of a-phase voltage and current, reference speed

Figure 6 shows initial states of torque change from to voltage and current, reference speed waveform.

5. Conclusions

This paper presents the sliding observer design scheme for electric vehicles under the varying load. The design procedures of the sliding mode have been established, which can be used to estimate vehicle speed and motor rotor flux. The simulation for the electric vehicle has been carried out using indirect vector control to observe the electric vehicle performance under varying parameter conditions. The simulation results meet the requirement of the SAE urban driving schedule B when correct parameter values are available. The results emphasize that the sliding mode observer can meet the SAE driving cycle velocity requirements.

References

[1] K. Rajashekara, "Propulsion System Strategies for Fuel Cell Vehicles.", *Fuel Cell Technology for Vehicles, PT-84,* Society of Automotive Engineers, Inc, 2000, pp. 179-187.

[2] P. T. Krein, R. Balog, "Low Cost Inverter Suitable for Medium-Power Fuel Cell Sources", *Power Electronics Specialists Conference*, 2002 IEEE 33rd Annual, June 2002, Vol. 1, pp. 321-326.

[3] R. Stobart, "Fuels for Fuel Cell-Powered Vehicles", *Fuel Cell Technology for Vehicles, PT-84,* Society of Automotive Engineers, Inc, 2000, pp. 61-67.

[4] N. Mohan, Tore M. Undeland, William P. Robbins, "Power Electronics Converters, Applications and Design", published by John Wiley & Sons, Inc., 1995.

[5] A. M. Tuckey, J. N. Krase, "A Low-Cost Inverter for Domestic Fuel Cell Applications", *Power Electronics Specialists Conference*, 2002 IEEE 33rd Annual, June 2002, Vol. 1, pp. 339-346.

[6] I. Husain, Electric and Hybrid Vehicles Design Fundamentals, CRC press LLC, 2003.

[7] L. J. Garces, "Parameter Adaptation for the Speed Controlled Static AC Drive with a Squirrel Cage Induction Motor", IEEE-IA Transaction, Vol. IA-16, No. 2, March/April, 1980, pp. 173-178.

[8] M. Koyuma et al, "Effects of Parameter Changes on Coordinate Control System of Induction Motor", Conference Record of the International Conference on Power Electronics, March, 1983, pp.684-695.

[9] D. W. Novotny, T. A. Lipo, Vector Control and Dynamics of AC Drives, Clarendon press, Oxford, 1996.

[10] I. Husain, M. S. Islam, "Design, Modeling and Simulation of an Electric Vehicle System", SAE International Congress and Exposition, Michigan, March 1-4, 1999.

[11] H.Kubota etal.,"DSP – Based Speed Adaptive Flux Observer of Induction motor", Vol.29, No2, pp344-348, 1993.

Induck Park received the B.S.E. E. from the Hanbat National University, Taejeon, Korea, the M.S.E.E. from Myongji University, Seoul, and Ph.D from Kongju National University in 1995, 1999, and 2005, respectively, all in electrical engineering. He is currently an Research Professor in the Department of Electrical Engineering, University ,Taejeon, Korea, engaged in teaching and research.

Sikyung Kim received the B.Sc. and M.S. degrees from Korea University, and the Ph.D degrees from Texas A&M University, College Station, U.S.A., in 1986, 1988, and 1994, respectively, all in electrical engineering.
He is currently a Professor in the Department of Electrical Engineering, Kongju National University ,Kongju, Chungnam, Korea, engaged in teaching and research.